Endovascular Aortic Aneurysm Repair with Stent-Grafts: Experimental Models Can Reproduce Endoleaks

Sophie Lerouge, PhD, Jean Raymond, MD, Igor Salazkin, MD, Zhao Qin, MSc, Louis Gaboury, MD, Guy Cloutier, PhD, Vincent L. Oliva, MD, and Gilles Soulez, MD, MSc

PURPOSE: To develop canine aneurysm models that can reproduce type II endoleaks after endovascular aneurysm repair (EVAR) with stent-grafts.

MATERIALS AND METHODS: A fusiform infrarenal abdominal aortic aneurysm model (AAA) was surgically created with a jugular vein patch, while preserving collateral vessels ($n = 3$). To allow comparative studies within the same animal, a bilateral iliac aneurysm model was also constructed with venous patches and surgical re-implantation of the sacroiliac trunk ($n = 3$). Stent-grafts were implanted by femoral approach at least 2 months later in both aortic and iliac models. Follow-up imaging was performed by Doppler ultrasound (US) and angiography until animals were killed 3 months after EVAR.

RESULTS: Angiography revealed immediate type II leaks in all cases. Leaks were still present at autopsy 3 months after EVAR in all cases, and were revealed at pre-death angiography in all but one case. At autopsy, leaks were characterized by the presence of large endothelialized channels that formed within the thrombus between the stent-graft and the aneurysmal wall.

CONCLUSION: As shown in this pilot study, persistent type II leaks after EVAR can be reproduced in aortic and iliac animal models. The iliac model can be created bilaterally in the same animal, thus allowing for comparative evaluation of different therapies. These models could be used to better understand the mechanisms of endoleak, and to assess future developments aimed to improve the outcomes after EVAR.

J Vasc Interv Radiol 2004; 15:971–979

Abbreviations: AAA = aortic aneurysm model, EVAR = endovascular aneurysm repair

ENDOVASCULAR aneurysm repair (EVAR) with stent-grafts is an alternative to bypass surgery for the treatment of abdominal aortic aneurysm (AAA) (1). EVAR is increasingly being used because of its less invasive nature and the growing prevalence of AAA in an aging population. One of the main drawbacks of this new technique is the persistence or recurrence of blood flow into the aneurysm after stent-graft placement, called endoleak, which occurs in 10% to 37% of patients (2–4). The most frequent are type I endoleaks, related to an ineffective seal at the graft ends, and type II endoleaks, associated with retrograde blood flow from collateral arteries (inferior mesenteric or lumbar arteries). Type I and II leaks occur in up to 10% and 10% to 25% of patients treated by EVAR, respectively (5). The mechanisms that cause or facilitate the development of endoleaks are poorly understood. Animal models are essential to allow a better understanding of these mechanisms, as well as to provide the appropriate tools to assess new strategies designed to decrease their occurrence. As such, there is a need to create an animal model that can reliably reproduce endoleaks (6,7). The goal of this pilot study was to develop two canine models that can reproduce type II endoleaks after stent-graft repair. The first model is an aortic model of sufficient size to implant stent-graft devices currently used in human AAA. The second model was developed in iliac arteries allowing comparative studies within the same animal.

From the Research Center (S.L., Z.Q., I.S., G.C.), Department of Radiology (G.S., J.R., V.O.), and Department of Pathology (L.G.), Centre Hospitalier de l'Université de Montréal, Notre-Dame Hospital, Montreal, Quebec, Canada. Received March 1, 2004; revision requested April 21; revision received and accepted April 23. Presented at the 2004 SIR Annual Meeting. **Address correspondence to** S.L., Research Center, JA de Seve Building, Notre-Dame Hospital, 1560 Sherbrooke East, Montreal, Quebec H2L 4M1, Canada; E-mail: sophie.lerouge@umontreal.ca

This project has been funded in part by the Plateforme Technologique du CHUM, Montreal, and by a structuring group grant from Valorisation Recherche Quebec. It now benefits from the CIRREF grant program.

G.S. is a consultant for Medtronic Canada Ltd. and has identified a potential conflict of interest. None of the other authors have identified a potential conflict of interest.

DOI: 10.1097/01.RVI.0000130816.33038.ED

MATERIALS AND METHODS

Surgical Construction of Aneurysms

AAA model.—All protocols for animal experimentation were approved by the institutional Animal Commit-

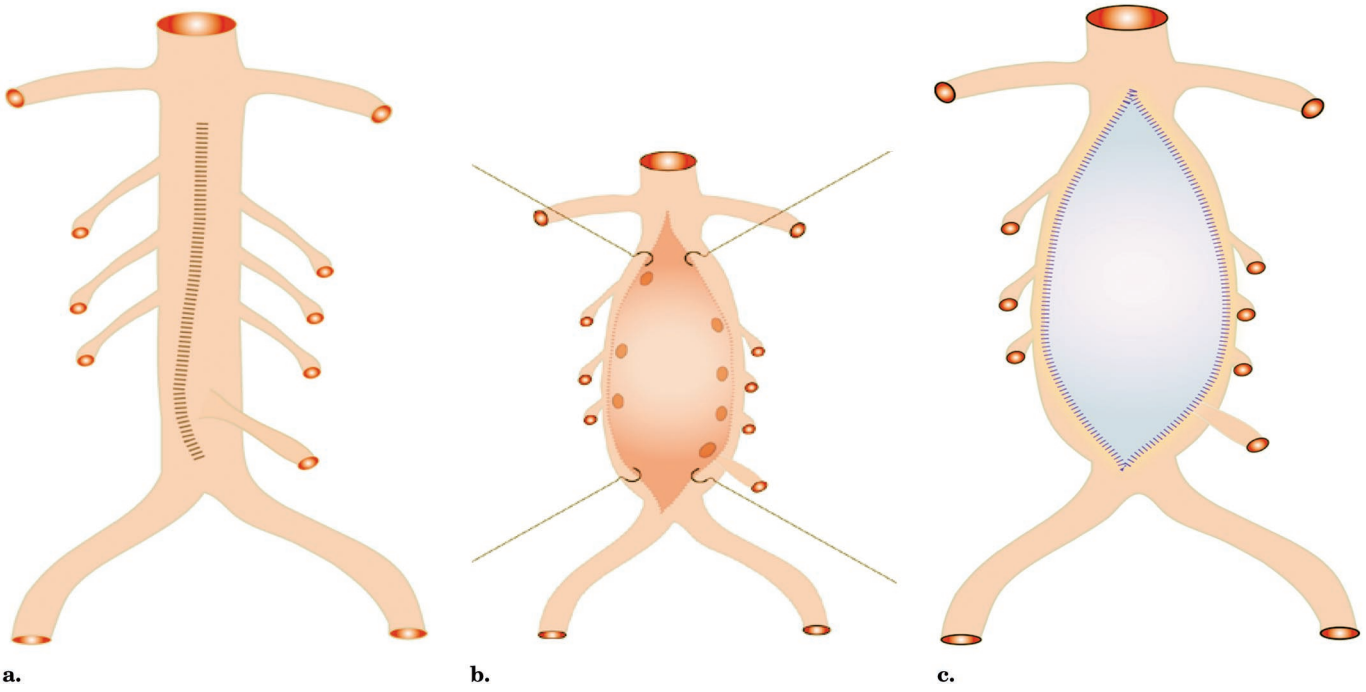

Figure 1. Abdominal aortic aneurysm model. Artistic representation showing construction of the AAA **(a–c)**. *(continues).*

tee in accordance with guidelines of the Canadian Council on Animal Care. Mongrel dogs were sedated with subcutaneous injection of acepromazine (0.1 mg/kg; Atravet, Ayerst Veterinary Laboratories, Guelph, ON, Canada), glycopyrrolate (0.01 mg/kg; Sabex Inc., Boucherville, QC, Canada), and meperidine (4 mg/kg; Sabex Inc.), and anesthetized with intravenous propofol (4 mg/kg; Diprivan 1%, AstraZeneca Canada, Montreal, QC, Canada). Animals were ventilated artificially and maintained with surgical anesthesia of 2% isoflurane. Postoperative analgesia was provided for 3 days by a 75 μg Fentanyl skin patch (Duragesic, Janssen-Ortho Inc., North York, ON, Canada).

AAAs were created in four mongrel dogs weighing 30 to 40 kg (**Fig 1a–d**). After the death of the first animal due to intra-abdominal sepsis, the protocol was changed to include the systematic use of female dogs, dental cleaning, and preoperative antibiotic therapy for 1 week. An external jugular vein was surgically exposed through a skin incision on the lateral surface of the neck, and an 8- to 10-cm-long segment was removed and placed into heparinized saline solution after proximal and distal ligation. The incision was closed in layers with 3.0 Vicryl. A midline laparatomy was performed and the exposure was maintained with mechanical retractors. Bowels were displaced from the abdominal cavity and protected with wet towels. The parietal peritoneum was dissected and the abdominal aorta was mobilized between renal and common iliac arteries. Temporary occlusion was achieved with large vascular clamps that included the orifice of all lumbar arteries. A 10-cm-long aortotomy was performed with scalpel and scissors. A venous patch shaped from the external jugular vein harvested from the same animal was positioned over the aortotomy and fixed with stay sutures. The anastomosis was completed with 4.0 Prolene running sutures. The operative site was packed, and blood flow restored. After thorough check for hemostasis and abdominal revision, intestines were repositioned and soft tissues closed in layers.

Iliac Model

In this study, three iliac aneurysms were surgically created in two mongrel dogs weighing 20 to 25 kg (**Fig 2a–d**). The iliac artery model was constructed in a similar fashion to AAA, except for the following details. A low midline laparatomy was performed. The peritoneum was dissected over common iliac arteries and the vessels were completely mobilized including the sacroiliac trunk. After flow arrest, a longitudinal arteriotomy was performed in midsection of the iliac arteries. To mimick the effect of a collateral, the sacroiliac trunk was transsected and sutured to the medial lip of the arteriotomy. A 45 mm patch fashioned from the external jugular vein of the same animal was positioned over the arteriotomy and sutured with continuously running 7.0 Prolene. In one dog, a fusiform aneurysm of 35 mm in length and 12 mm in diameter was created. In the second animal, bilateral iliac aneurysms were made shorter (17 mm) and larger (17–18 mm).

Endovascular Interventions and Creation of Type II Leaks

Stent-graft implantation was performed 8 weeks after surgery. In the AAA model, Talent iliac stent-grafts (12 mm nominal diameter; 115–145 mm long with a 13-mm proximal bare stent) (Medtronic; Santa Rosa, CA) consisting of a thin Dacron monolayer

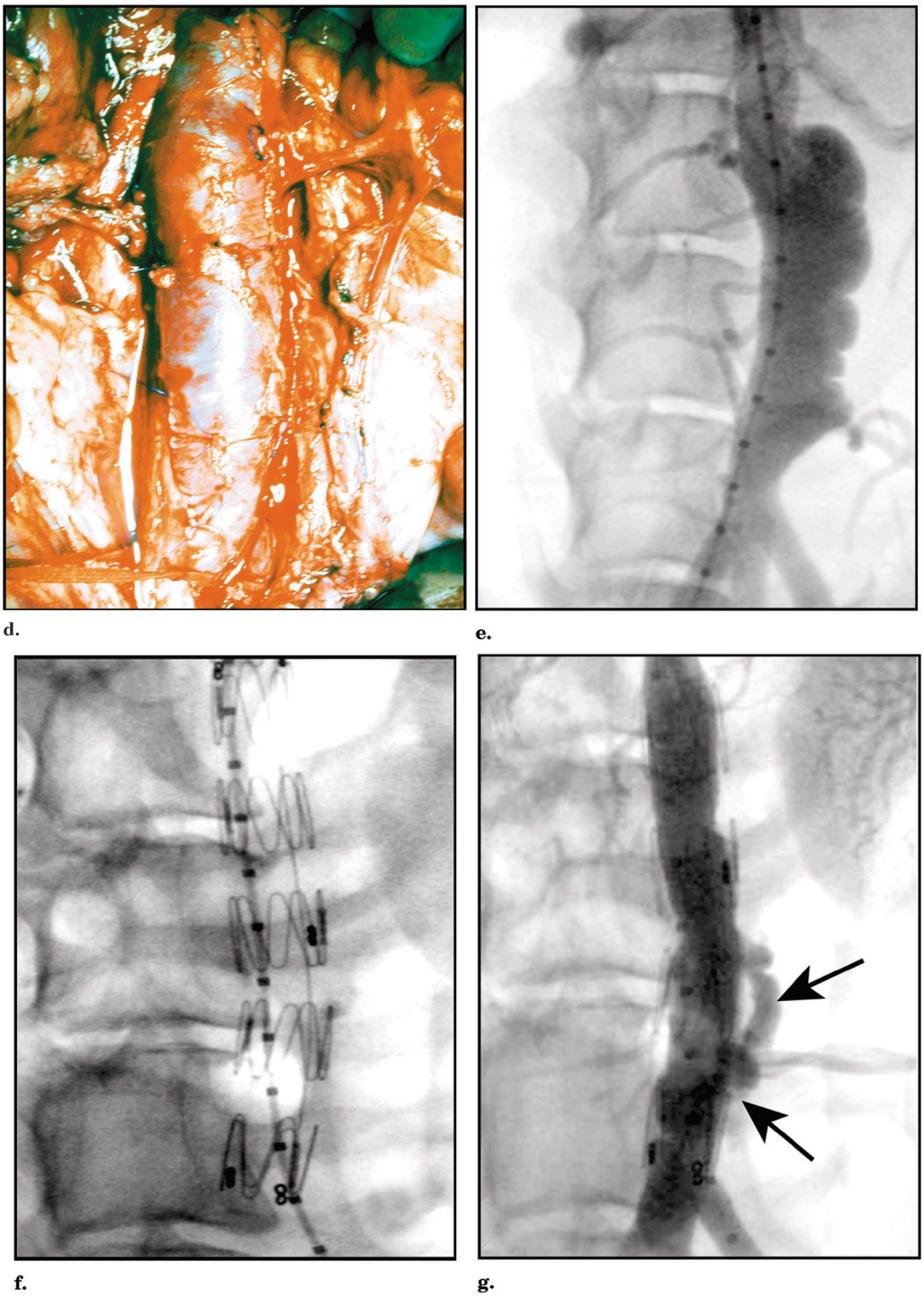

Figure 1. *(continued)* A peroperative photograph shows resulting fusiform aneurysm **(d)**. Angiography 8 weeks after surgery, immediately before **(e)** stent-graft implantation **(f)**, showing type II leak 3 months later **(g)**.

sutured to a NiTi support, were implanted with fluoroscopic guidance, an 18-F catheter, and standard clinical endovascular techniques and surgical exposition of the femoral artery (n = 3). In the iliac aneurysm model, balloon expandable Jostent stent-grafts (diameter, 4–9 mm; length, 48 mm) (Jomed, Rangendingen, Germany), were implanted with fluoroscopic guidance in the fusiform aneurysms (n = 3). The Jostent stent-graft consists of a polytetrafluoroethylene graft sandwiched between two stainless steel structures. Implants were deployed

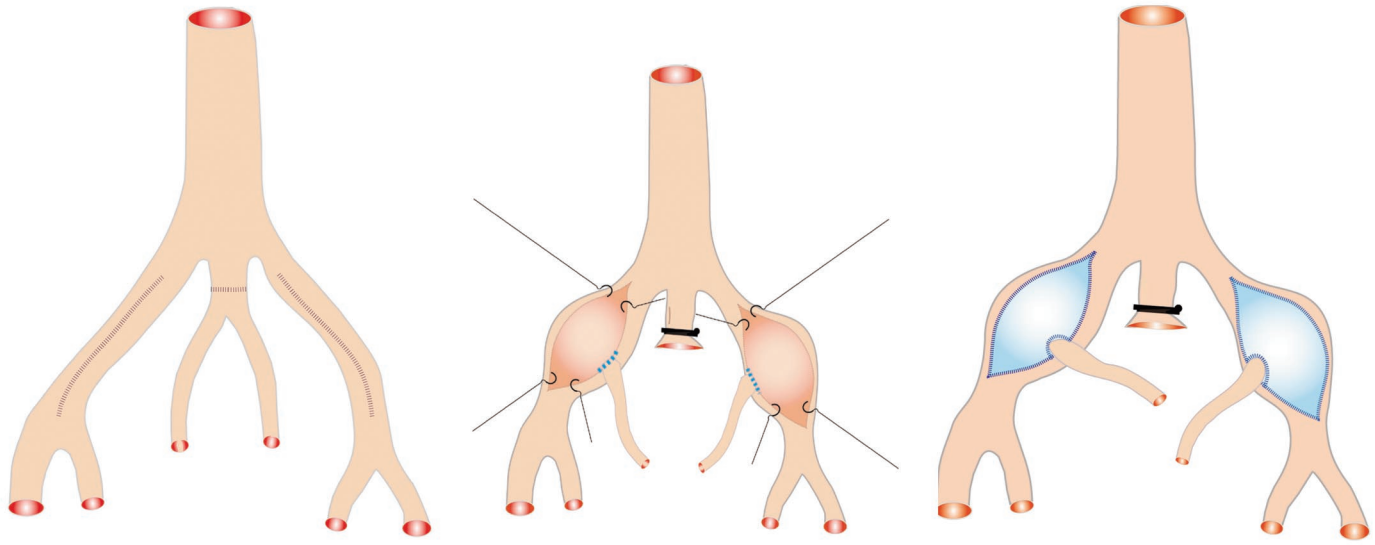

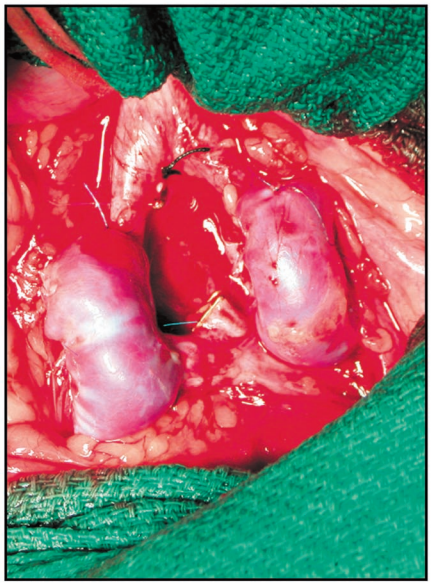

Figure 2. Iliac aneurysm model. Artistic representation of the surgical construction of bilateral iliac aneurysms **(a–c)**. A peroperative photograph shows resulting fusiform aneurysms **(d)** *(continues)*.

and expanded at 110% of the nominal diameter (6 mm).

Follow-up Imaging

Follow-up imaging was performed with Doppler ultrasound (US) with a 10 MHz probe (Vivid 5, GE Vingmed, Horten, Norway) 2 days after surgery and 48 hours, 3 weeks, and 3 months after stent-graft implantation. Percutaneous transfemoral angiography was obtained at the time of stent-graft implantation and before animal killing at 3 months. Both imaging modalities were used for the detection and classification of endoleaks and for assessing graft patency. At angiography, type II endoleaks were defined as residual opacification of aneurysms, through retrograde flow from one of the collateral vessels in abdominal aneurysms (AAA model) or from the surgically re-implanted sacroiliac trunk (iliac model). In addition to the evaluation of endoleak, Doppler sonography was used to detect changes in aneurysm size over time, by recording diameters at the proximal, medial, and distal thirds of the aneurysm.

Histopathology

Three months after stent-graft implantation, the dogs were killed by barbiturate overdose immediately after angiography. The aorta and iliac arteries were harvested "en bloc" and fixed in buffered formalin. The Exakt cutting-grinding system (Exakt Gmbh, Norderstedt, Germany) was used to prepare histological slides including the tissue/stent-graft interface. The explants were frozen in liquid nitrogen and cut with the Exakt diamond saw into transverse sections at the

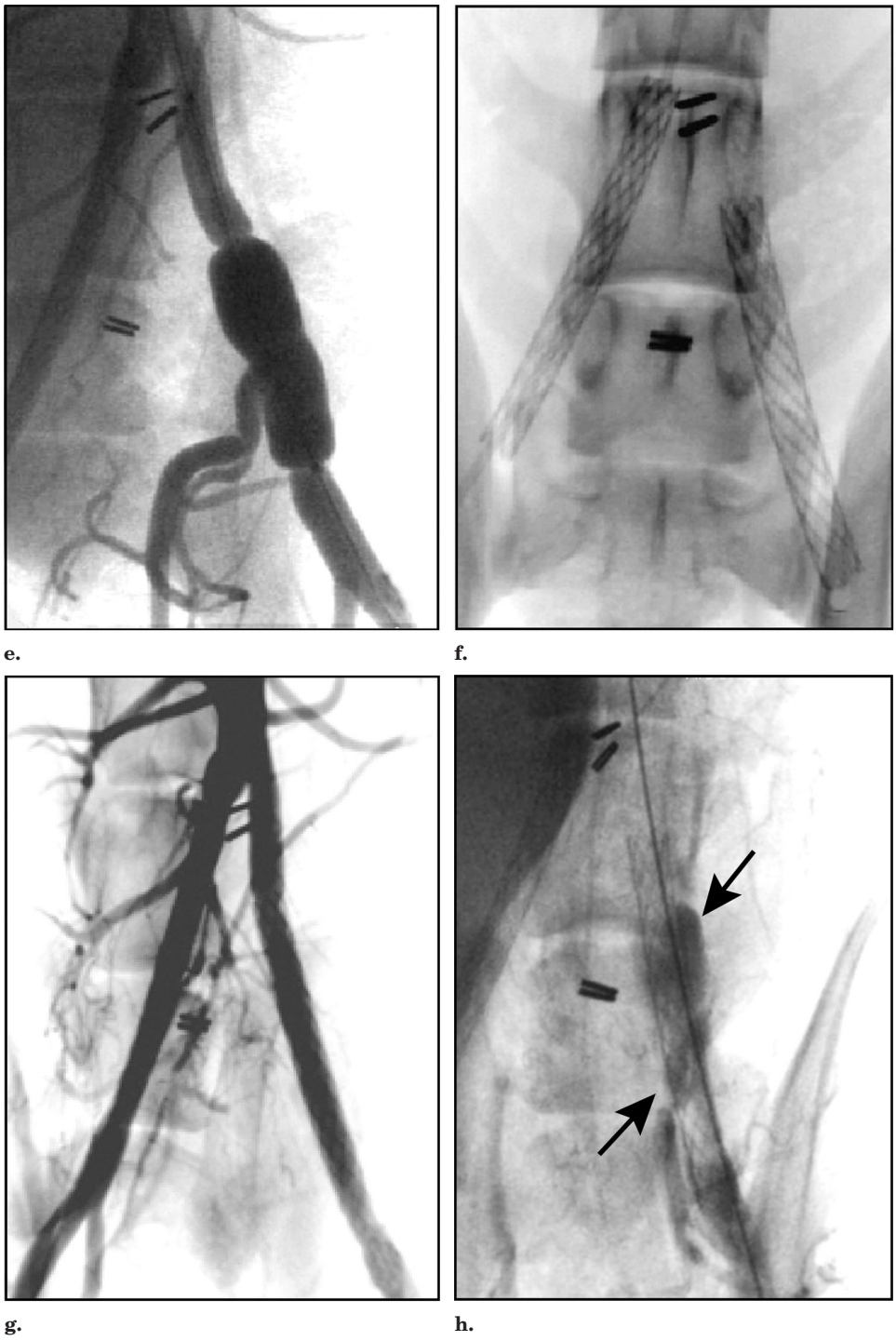

Figure 2. *(continued).* Angiograms before **(e)** and after stent-graft implantation **(f–h)** in a left iliac aneurysm demonstrate exclusion of the aneurysm by the graft **(g)** but retrograde opacification through implanted collateral **(h, arrows)**.

proximal and distal necks and proximal, medial, and distal thirds of the aneurysm, which were analyzed and photographed. Tissues were dehydrated and embedded in an acrylic resin (Technovit 7200), cut and polished by successive grinding papers into 20 to 30 μm sections that were then stained by hematoxylin and eosin. For better identification of cells, the implant was carefully removed from a few transverse sections to prepare conventional 3-μm-thick, paraffin-embedded slides of the surrounding thrombus that were stained by

Aneurysm Size and Changes Over Time in Both Canine Models

Dog	Model	SG	Angiographic Endoleaks		Length of Aneurysm (mm)	Mean Aneurysm Diameter (mm) (% diameter at surgery)			
			EVAR	Sacrifice		Surg	EVAR	3 Weeks	Sacrifice
1	AAA	Animal sacrificed 3 days post-surgery				NA	NA	NA	NA
2	AAA	Talent	II	II	80	19.6	22.8 (116)	22.6 (115)	21.9 (112)
3	AAA	Talent	II	—	100	22.1	29.0 (131)	30.9 (140)	27.3 (123)
4	AAA	Talent	II	II	80	18.8	21.7 (116)	24.5 (131)	25.0 (133)
5	Iliac LI	Jostent	II	II	35	10.7	12.1 (110)	11.9 (108)	9.7 (88)
6	Iliac LI	Jostent	II	II	18	14.0	16.3 (116)	—	10.8 (92)
7	Iliac RI	Jostent	II	II	17	11.6	12.6 (109)	—	10.7 (93)

Note.—Aneurysm diameter was calculated as the average between measurements at the proximal, medial and distal thirds of the aneurysm by ultrasound imaging (in brackets, diameter at follow-up, expressed as the percentage of diameter after surgery). Depending on the model, Talent iliac SG (Medtronic, USA) or Jostent SG (Jomed, Germany) were implanted in the aneurysm. RI = right iliac; LI = left iliac; SG = stent-graft; II = type II endoleaks.

Movat pentachrome or with immunohistochemistry. The presence of endothelial cells was confirmed by immunohistochemistry staining with factor VIII.

RESULTS

In the three animals surviving AAA surgery, infrarenal abdominal aortic aneurysms measuring 87 mm (±12 mm) in length and 20 mm (±2 mm) in diameter were created (**Fig 1**). Angiography and Doppler US showed the presence of type II endoleaks in these three dogs immediately after stent-graft implantation. Leaks persisted at 3-month angiography in two of three dogs (**Fig 1**). In the third dog, a leak was detected at angiography and US at 3 weeks but not at 3 months; however, evidence of a leak was found at pathology after death. In iliac aneurysms, type II leaks were identified immediately after EVAR and persisted until death in all cases (**Fig 2**). All grafts remained patent. The evolution of aneurysm diameter over time is detailed in the **Table**. Mean diameters were obtained by averaging sonographic measurements obtained at the proximal, medial, and distal thirds of the aneurysm. Aneurysm size increased between surgery and stent-graft implantation (mean, 16% ±7%). After EVAR, the diameter of AAAs increased slightly or stabilized, whereas a slight decrease of the iliac aneurysms was observed (**Table**). Aside from endoleak pockets, tissue between the stent-graft and aneurysmal wall presented heterogeneous areas of iso- and hypoechoic signal at US examination.

Incomplete organization into connective tissue and presence of large endothelialized channels were the two main patterns observed on histological analysis of the surrounding thrombus. Areas of fibrin and red blood cells alternated with more or less organized connective tissue, generally near the vessel wall, where fibroblasts, actin-positive cells and numerous small neovessels were present. Very poorly organized regions were still present near the stent-graft 3 months after EVAR in the AAA model, whereas better tissue organization was seen in the iliac model. In all aneurysms, one or several macroscopic "pseudovascular" channels, measuring a few millimeters in caliber and lined with endothelial cells, were observed between the graft and the aneurysmal wall, as confirmed by factor VIII immunohistochemical staining (**Fig 3**). In the iliac model, a connection with the collateral vessel could be confirmed.

Histological analysis also showed that stent-graft incorporation into a mature neointima was limited to regions where the implant was close to the vessel wall (proximal and distal necks, posterior region near the ends of the aneurysm), while only immature neointima or intraluminal thrombus were observed at other locations such as the middle of the aneurysm. Moreover, neointimal continuity was not always present at the ends of the stent-grafts, particularly at the transition zone between the bare and covered portions of the Talent (Medtronic) stent-graft.

DISCUSSION

The mechanisms leading to endoleaks after EVAR are poorly understood. The development of an AAA animal model reproducing endoleaks is an important step for the study of mechanisms and exploration of potential solutions to prevent endoleaks. Large animals are required to study clinically applicable endovascular tools and their modifications. Aneurysm models created by overdilatation with balloon inflation with/without elastase infusion, or by surgery with venous/arterial patch, have already been described (6,8–14). However, these have been generally used for device testing, and none have proved to reproduce endoleaks. Recently Pavcnik et al intended to create chronic type II leaks with a patch from the inferior vena cava on the abdominal aorta with insertion of perforated stent-graft to create an arteriovenous fistula (6). However, this model did not reliably produce type II leaks.

This study presents two canine models that can reproduce chronic type II endoleaks after EVAR. These leaks appear immediately after EVAR and depend on circulation established by the driving gradient created between systemic and aneurysmal sac pressures, when there is a good seal between the stent-graft and the vessel wall at the aneurysmal necks. The authors believe that key factors for successful production of endoleaks here

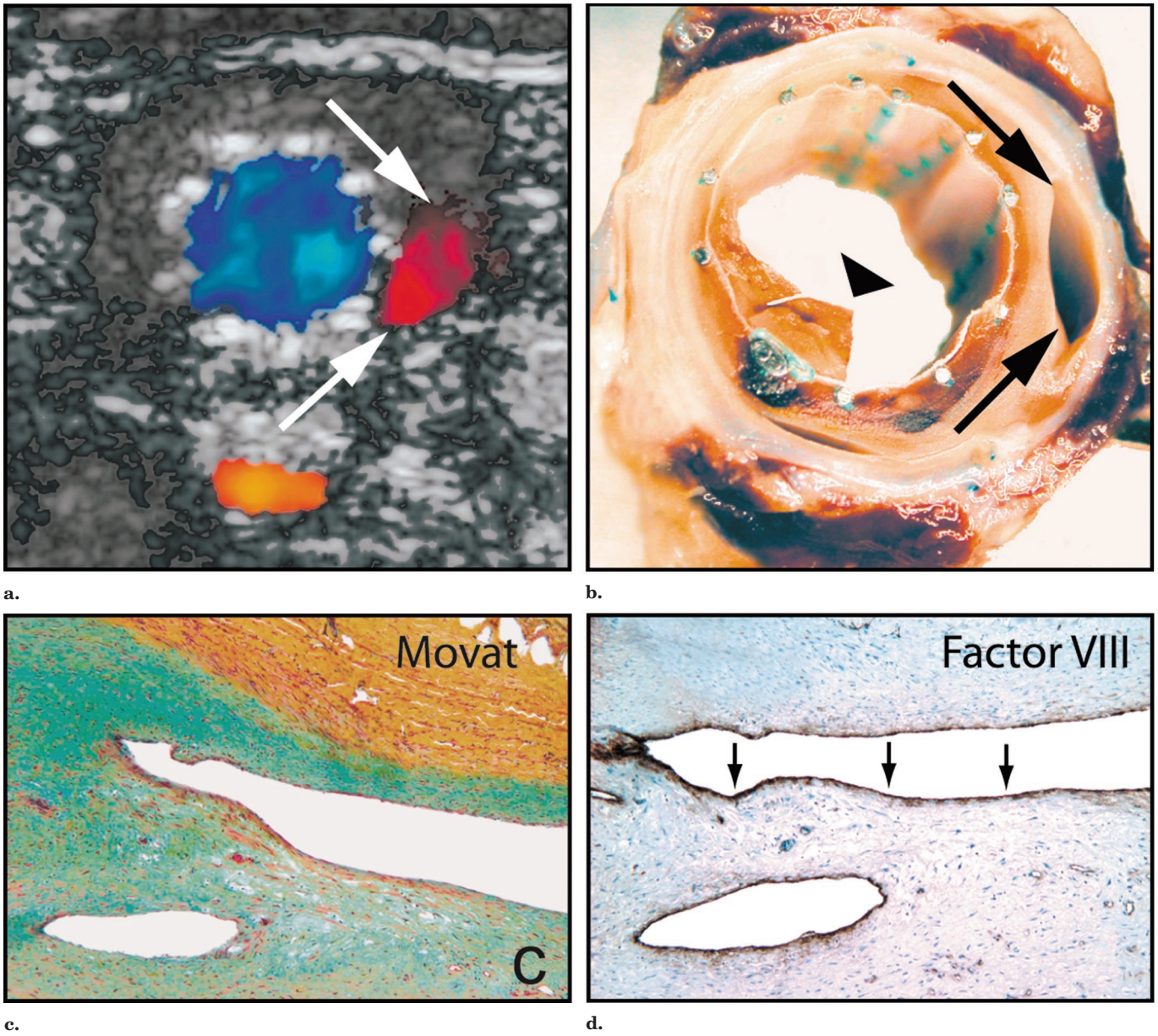

Figure 3. Type II endoleaks. Type II endoleaks are structures that present residual flow as shown by color Doppler sonography in **(a)**. They are located outside the stent-graft but within the organized aneurysmal thrombus. **(b)** A macrophotograph of an aortic transverse section shows a type II endoleak (arrows) as well as endoluminal thrombus (arrowhead). **(c)** The endoleak is generally found within organized connective tissue (Movat's pentachrome stain; ×50 original magnification). **(d)** It is lined by factor VIII positive cells (arrows) (immunostain for factor VIII; ×50 original magnification).

were the length of the patch in the AAA model, which allow keeping several collaterals patent and the surgical creation of a patent "collateral" in the iliac model. An additional consideration in the success of the model is the choice of animal species: aneurysms created in canine models tend to persist, whereas aneurysms crated in porcine models have a propensity to thrombose and heal spontaneously (15). Dogs were also shown to more closely reproduce poor incorporation of human implants, whereas pigs tended to heal with exuberant neointimal formation (7–8,15–17). Among large animals, canine models present the best morphological and tissue healing characteristics (7), as suggested by the Ad Hoc Committee of the Society for Vascular Surgery and for Cardiovascular Surgery.

Angiographic endoleaks were observed in three of three iliac aneurysms and in two of three AAAs at 3 months. In the third case of abdominal aneurysm, an endoleak type II was

present after implantation, but it was no longer visible at angiography before death; yet, signs of on-going blood perfusion and the presence of a "pseudovascular" channel were observed at pathology. The authors believe that a small leak was present at 3 months but was not detected by angiography. Computed tomography (CT) scan, which is recognized as the most efficient method (18), may have allowed its detection. The number of animals in this experimentation was too small to draw any conclusion on the variation of AAA diameter during follow-up Doppler US.

Histopathological analysis of these models may be helpful to better understand the mechanisms of endoleaks. Recent studies of specimen retrieved at autopsy or late surgical conversion after EVAR (19–21) reported poor tissue organization around the implant, even months or years after its implantation. The lack of a mature neointima incorporating the stent-graft into the vessel wall, the stent-graft being easily separated from the aorta and the aneurysmal sac, was observed by several authors (19,20). They concluded that attachment of presently commercialized stent-graft is purely or mostly mechanical. Moreover, the surrounding thrombus seems to be an immature, heterogeneous, often semi-liquid tissue (19,21). These data suggest that healing around the implant is insufficient to ensure complete exclusion of the aneurysm from blood flow coming from the aorta or collaterals. The pathology of our animal models at 3 months reproduced some of these findings at autopsy, such as endoluminal thrombus, poor perigraft organization, and lack of stent-graft incorporation by neointimal growth in the aneurysmal sac.

The presence of large channels lined with endothelial cells within the surrounding thrombus of all dogs indicates that these could play an important role in the persistence of endoleaks. Even when the thrombus surrounding the implant is completely organized into connective tissue, such channels allow persistence of circulating blood into the aneurysm and their spontaneous thrombosis is not to be expected. The origin of endothelial cells (intima or vasa vasorum of the aneurysmal pouch, native or collateral artery, and/or circulating progenitor cells (22,23), etc.) and the mechanisms of formation of these channels remain to be clarified.

Respective advantages of these aortic and iliac models include the ability to test the performance of large commercial implants in relation to type II endoleaks in the former, and the possibility of obtaining comparative bilateral studies with paired data in the latter model. The inability to identify a type II leak at angiography in one of the three animals with the aortic model represents a limitation. Given its superior contrast resolution, CT would be the ideal tool to identify and follow the presence of leaks in these animals. These experimental models differ from conditions encountered in patients who develop AAA, such as irregular aneurysm necks, calcified plaques, and frequent intraluminal thrombus, and their validity and reproducibility need to be further assessed. Yet, they are promising tools to improve the understanding of mechanisms that cause endoleaks and to evaluate the impact of future modifications of stent-graft implants or implantation techniques on their occurrence.

Acknowledgments: The authors thank Jocelyne Lavoie (endovascular procedure and planification), Hélène Héon (veterinarian), and Cédric Schmitt (US image management) for their participation in the animal studies, Guylaine Gevry for her assistance with artwork, and Dr. Guy Allaire, Dr. Lydia Whady, and Robert Spenard, from the Department of pathology of CHUM, for access to histological equipment.

References

1. Uflacker R, Robison J. Endovascular treatment of abdominal aortic aneurysms: a review. Eur Radiol 2001; 11: 739–753.
2. Dattilo JB, Brewster DC, Fan CM, et al. Clinical failure of endovascular aortic repair: incidence, causes and managements. J Vac Surg 2002; 35:1137–1144.
3. Schurink GW, Aarts NJ, van Bockel JH. Endoleak after stent-graft treatment of abdominal aortic aneurysm: a meta-analysis of clinical studies. Br J Surg 1999; 86:581–587.
4. White GH, Yu W, May J, Chaufour X, Stephen MS. Endoleak as a complication of endoluminal grafting of aortic aneurysms: classification, incidence, diagnosis, and management. J Endovasc Surg 1997; 4:152–168.
5. Veith FJ, Baum RA, Ohki T, et al. Nature and significance of endoleaks and endotension: summary of opinions expressed at an international conference. J Vasc Surg 2002; 35:1029–1035.
6. Pavcnik D, Andrews RT, Yin Q et al. A canine model for studying endoleak after endovascular aneurysm repair. J Vasc Interv Radiol 2003; 14(10):1303–1310.
7. Carrell TW, Smith A, Burnand KG. Experimental techniques and models in the study of the development and treatment of abdominal aortic aneurysm. Br J Surg 1999; 86:305–312.
8. Lambert AW, Budd JS, Fox AD, et al. The incorporation of a stent-graft into the porcine aorta and the inflammatory response to the endoprosthesis. Cardiovasc Surg 1999; 7:710–714.
9. Palmaz JC, Tio FO, Laborde JC, et al. Use of stents covered with polytetrafluoroethylene in experimental abdominal aortic aneurysm. J Vasc Interv Radiol 1995; 6:879–885.
10. Eton D, Warner DL, Owens C, et al. Results of endoluminal grafting in an experimental aortic aneurysm model. J Vasc Surg 1996; 23:819–831.
11. Benson AE, Palmaz JC, Tio FO, Sprague EA, Encarnacion CE, Josephs SC. Polytetrafluoroethylene-encapsulated stent-grafts: use in experimental abdominal aortic aneurysm. J Vasc Interv Radiol 1999; 10:605–612.
12. Maynar M, Qian Z, Hernandez J, et al. An animal model of abdominal aortic aneurysm created with peritoneal patch: technique and initial results. Cardiovasc Intervent Radiol 2003; 26: 168–176.
13. Wu MH, Shi Q, Bhattacharya V, Sauvage LR. Development of a symmetric canine abdominal aortic aneurysm model with clinical relevance for endovascular graft studies. J Invest Surg 2001; 14:235–239.
14. Soula P, d'Othee BJ, Otal P, et al. Macroporous polyester-covered stent in an experimental abdominal aortic aneurysm model. J Endovasc Ther 2001; 8:390–400.
15. Desfaits AC, Raymond J, Muizelaar J. Growth factors stimulate neointimal cells in vitro and increase the thickness of the neointima formed at the neck of porcine aneurysms treated by embolization. Stroke 2000; 31:498–507.
16. Raymond J, Venne D, Allas S, et al. Healing mechanisms in experimental aneurysms. I. Vascular smooth muscle cells and neointima formation. J Neuroradiol 1999; 26:7–20.
17. Venne D, Raymond J, Allas S, et al. Healing of experimental aneurysms. II: Platelet extracts can increase the thickness of the neointima at the neck of treated aneurysms. J Neuroradiol 1999; 26:92–100.
18. Golzarian J, Struyven J. Imaging of

complications after endoluminal treatment of abdominal aortic aneurysms. Eur Radiol 2001; 11:2244–2251.
19. Malina M, Brunkwall J, Ivancev KM, et al. Endovascular healing is inadequate for fixation of Dacron stent-grafts in human aortoiliac vessels. Eur J Vasc Endovasc Surg 2000; 19:5–11.
20. McArthur C, Teodorescu V, Eisen L, et al. Histopathologic analysis of endovascular stent grafts from patients with aortic aneurysms: does healing occur? J Vasc Surg 2001; 33:733–738.
21. White RA, Walot I, Donayre CE, Woody J, Kopchok GE. Failed AAA endograft exclusion due to type II endoleak: explant analysis. J Endovasc Ther 2001; 8:254–261.
22. Asahara T, Masuda H, Takahashi T, et al. Bone marrow origin of entdothelial progenitor cells responsible for postnatal vasculogenesis in physiological and pathological neovascularization. Cir Res 1999; 85:221–228.
23. Tepper OM, Sealove BA, Murayama T, Asahara T. Newly emerging concepts in blood vessel growth: recent discovery of endothelial progenitor cells and their function in tissue regeneration. J Investig Med 2003; 51:353–359.